Original Article

Tumor Biology

Tumor Biology
March 2017: 1–12

DOI: 10.1177/1010428317695530
journals.sagepub.com/home/tub
SAGE

Ganoderic acid targeting nuclear factor erythroid 2–related factor 2 in lung cancer

Balraj Singh Gill[1], Sanjeev Kumar[2] and Navgeet[3]

Abstract

Lung cancer causes huge mortality worldwide, and targeting new pathway may provide an alternative in modulating signaling in cancer. Nuclear factor erythroid 2–related factor 2 is the major regulator of endogenous and exogenous stress by activating numerous antioxidant genes critical in cancer, Alzheimer's, Parkinson's, and inflammatory bowel diseases. Ganoderic acid is a triterpene from basiodiomycetes fungus *Ganoderma lucidum* with numerous therapeutic effects. In this study, ganoderic acid and its 50 isomers and natural activators were docked by receptor-based molecular docking using Maestro 9.6 (Schrödinger Inc.) in the Kelch-like ECH-associated protein 1-nuclear factor erythroid 2–related factor 2 signaling pathway. The receptor-based molecular docking reveals the best binding interaction of nuclear factor erythroid 2–related factor 2 and ganoderic acid A with GScore (−9.69) (kcal/mol), Lipophilic EvdW (−1.83), Electro (−0.72), Glide emodel (−73.369), H bond (−1.1), molecular mechanics/generalized Born surface area (−75.541) with Leu 718, Asp 800, Cys 797 residues involved in hydrogen bonding. The calculated docking energy highlights the lipophilic, hydrogen bonding, pi–pi stacking interactions, and non-covalent bonding. Analysis showed the involvement of cysteine and serine residues which were crucial in the activation and translocation from cytoplasm to the nucleus in the nuclear factor erythroid 2–related factor 2 signaling process. The molecular docking tool QikProp analyzed the absorption, distribution, metabolism, excretion, and toxicity but needs some modifications in their structure to satisfy Lipinski's rule. Ganoderic acid A is a best docked isoform which inhibits the cell proliferation, viability, migration, and reactive oxygen species and messenger RNA expression of nuclear factor erythroid 2–related factor 2 in H460 cells.

Keywords

Nuclear factor erythroid 2–related factor 2 signaling, cancer, ganoderic acid, molecular docking, antioxidant

Date received: 13 November 2016; accepted: 11 January 2016

Introduction

Lung cancer causes huge mortality worldwide, mainly among smokers and few among non-smokers. Non-small-cell lung carcinoma (NSCLC) is common cancer among smokers, and non-smokers focus on its specific subtypes, squamous cell carcinoma or adenocarcinoma (AC). The reactive oxygen and nitrogen species causes oxidative stress and prove to be harmful, whereas controlled level of oxidant regulates signaling pathways.[1] The defense system is counterbalanced by oxidant system using different mechanisms regulating physiology of the body. The Kelch-like erythroid-derived Cap-n-Collar Homology (ECH)-associated protein 1 (Keap1)-Nrf2 pathway is the main regulator of cytoprotective responses caused by reactive oxygen species (ROS). Nuclear factor erythroid 2–related factor 2 (Nrf2) is the transcription factor which under normal condition remains in the cytoplasm with the association of Keap1 and Cullin 3 proteins which degrade Nrf2 ubiquitination.[2] Keap1 is a cysteine-rich protein substrate adapter which promotes Cullin 3 to ubiquitinate Nrf2. The process of degradation ubiquitinated the Nrf2 and

[1]Centre for Biosciences, Central University of Punjab, Bathinda, India
[2]Centre for Plant Sciences, Central University of Punjab, Bathinda, India
[3]Department of Biotechnology, Doaba College, Jalandhar, India

Corresponding author:
Balraj Singh Gill, Centre for Biosciences, Central University of Punjab, Bathinda 151001, India.
Email: gillsinghbalraj@gmail.com

recycled by translocation of the proteasomes. Oxidative stress conditions disrupt the cysteine residues in Keap1, which results in disruption of Keap1-Cul3 ubiquitination system.[3] Non-ubiquitination of Nrf2 results in the accumulation in the cytoplasm which further translocates it into the nucleus. In the nucleus, it forms a complex with small transcription factor (Maf) protein that binds to the promoter region of antioxidant response element (ARE) of antioxidative genes which initiates cascade for activation of transcription.[4] Activation of Nrf2 pathway leads to NAD(P)H-quinone oxidoreductase 1 (Nqo1), glutamate–cysteine ligase, sulfiredoxin 1 (SRXN1), and thioredoxin reductase 1, glutathione S-transferase (GST), and uridine 5′-diphospho-glucuronosyltransferase (UDP)-glucuronosyltransferase (UGT). ROS are mutagenic and may thereby promote cancer.[5] Activation of Nrf2 signaling protects against cancer, aging, diabetes, cardiovascular disease, neurodegenerative diseases, inflammation, pulmonary fibrosis, and acute pulmonary injury.[6] Different natural products such as quercetin,[7] curcumin,[8] ursolic acid,[9] and celastrol[10] have potential to modulate Nrf2 signaling cascade.[11] One of the neglected natural products is *Ganoderma lucidum*, used as medicine since ancient time, hence known as herb of spirtual potency.[12,13] Previously, our research group carried out the anticancer property of *G. lucidum* and active compounds in different signaling pathways in cancer. The methods use in this study was taken from our previous studies.[14–16] Among different bio-constituents in *G. lucidum*, ganoderic acid was explored for revealing mechanism in cancer signaling.[17] In this study, molecular docking was performed for the first time on Nrf2 with 50 isoforms of ganoderic acid and their natural inhibitors to reveal the mechanistic binding of Keap1-Nrf2 pathway. After molecular docking, best isoforms of ganoderic acid on the basis docking score was checked for the biological activity in the cell line.

Methodology

Preparation of ligands and protein molecule

The three-dimensional structure of protein crystallized structure was downloaded from Protein Data Bank (PDB) site with Nrf2 (PDB: 4L7D)[18] from which water molecules were removed in concern to the domain topology that usually interacts with hydrophobic regions. Subsequently, polar hydrogen, wherever required, were incorporated to fill the inappropriate valency of the protein atoms, ensuing in increased polarizability of bonds. The increased polarizability enhanced the probability of ligand–protein interactions. Later, processed protein structure was checked for the stereochemical quality by residue-by-residue geometry as well as overall structural geometry. The preparation of different isoforms of ganoderic acid and other natural activator structures was carried out by software ChemBioDraw Office[17] (licensed at Cambridge's soft). Literature survey highlighted that some of the natural activators such as quercetin,[7] curcumin,[8] ursolic acid,[9] and celastrol[10] target the Nrf2 signaling. These compounds were subjected in the LigPrep for the ligand preparation by Maestro 9.3. LigPrep was corrected by addition and optimization of hydrogen bonds for correcting the valency, creation of disulfide bonds, and fixing of missing residues. These modifications prepares the ligands prior to the docking. Furthermore, prepared structure was minimized and optimized with liquid simulations (OPLS-2005) force field to acquire an energetically stable geometry.[19–22]

Receptor grid formation

Grid pre-calculates grid maps of interaction energies by scoring electrostatic, dispersive energies of surrounding target with a macromolecule before the docking.[17] The grid maps are used to determine the total interaction energy for a ligand with a macromolecule. Grid mapping computes the crucial coordinates data and assigns the coordinates of the Nrf2 prior to the receptor based docking. Furthermore, grid mapping affords an appropriate surface topology for the ligand atoms for interaction with the Nrf2 domain. Grid mapping is a pre-requisite to direct various isoforms of ganoderic acids to bind for their region of the firm affinity of the Nrf2 domain. Grid results in favorable interaction and best post during binding which represents conformation, position, orientation in the receptor-ligand complex. Other parameters such as sites, constraints, rotatable groups, and excluded volume, which are the default settings of the Maestro 9.6, are used.[23]

Glide receptor based molecular docking

Molecular docking procedures were carried out after preparing the ligand, protein, and the grid on the active site of the protein. Glide docking tools predict the systematic and computational simulation method for predicting best binding orientation to the protein target. Glide molecular docking outputs GScore (empirical scoring function) which is a combination of various parameters relevant to binding energy. The GScore is calculated by calculating ligand–protein interaction energies, root mean square deviation (RMSD), hydrogen bonds, hydrophobic interactions, internal energy, pi–pi stacking interactions, and desolvation.[17] Glide module of the XP visualizer analyzes the specific ligand–protein interactions. Ligands were docked with the X-ray crystal structure of Nrf2 (PDB: 4L7D) using Glide. The best possible fit compounds' results after docking were analyzed for thermodynamic optimal energy value, the potential of bonding and conformations, types of interactions, residues involved in the interaction, and the distance between different residues.[24,25]

Prime/molecular mechanics/generalized Born surface area simulation (free energy calculation)

The proper solvation facilitates in the process of molecular recognition. The solvation effect estimates the binding affinities by molecular mechanics/generalized Born surface area (MM-GBSA) scoring, where MM means molecular mechanics, GB means Generalized Born, and SA means solvent-accessible surface area. In MM-GBSA simulation, electrostatics of ligand–receptor complex and solvation were analyzed which has the edge over prior methods of Coulomb-based terms. The Prime/MM-GBSA approach calculates free energy and calculates the binding affinity of the receptor and the ligands.[26] The simulation was based on the structure obtained by receptor-based ligand molecular docking. The ligand poses were minimized by Prime, whereas energy of the complex was obtained by OPLS-2005 force field with VSGB2.0 solvent model in GB/surface area continuum solvent model[27]

$$\Delta G_{bind} = \Delta_E + \Delta G_{solv} + \Delta G_{SA}$$

$$\Delta E = E_{complex} - E_{protein} + - E_{ligand}$$

where ΔE is the minimized energy of complex, protein, and ligand.

$$\Delta G_{solv} = G_{solv(complex)} - G_{solv(protein)} - G_{solv(ligand)}$$

where ΔG is the solvation free energy of the complex protein and ligand.

$$\Delta G_{SA} = G_{SA(complex)} - G_{SA(protein)} - G_{SA(ligand)}$$

where ΔGSA is surface area energy of the complex protein and ligand.

Absorption, distribution, metabolism, and excretion properties

QikProp is an important tool that calculates properties of the significant descriptors and pharmaceutically relevant molecules by comparing their values with those of 95% of already known pharmaceutical drugs. Absorption, distribution, metabolism, excretion, and toxicity (ADME-T) properties of the docked ligand molecules were subjected to QikProp tool. It analyzes and predicts different properties of drugs, about the use and aftermath of drug intake, that is, ADME. It gives the information about QPlogPo/w, QPlogBB, overall central nervous system (CNS) activity, Caco-2, Madin–Darby Canine Kidney (MDCK) cell permeability, logKhsa for human serum albumin binding, and the percentage of human oral absorption.[28]

Materials and methods

Ganoderic acid A (≥98%) was purchased from Sigma-Aldrich and dissolved in dimethyl sulfoxide (DMSO) at a concentration of 50 mM and stored at −20°C. Lung cancer cell line (H460) used in the study was procured from National Centre for Cell Sciences, Pune, India. The cell line was carefully maintained in RPMI media supplemented with 10% heat-inactivated fetal bovine serum (FBS), 1% penicillin (units/mL), streptomycin (100 mg/mL). Cells were maintained at 37°C in a humidified atmosphere with 5% CO_2.

Total RNA isolation, complementary DNA synthesis, and reverse transcription-polymerase chain reaction

About one million cells were seeded and supplemented with culture media having 10% FBS and 1% penicillin/streptomycin, incubated at 37°C. H460 cells were treated with 80 µM of ganoderic acid for 48 h, and then, total RNA was isolated and extracted using Trizol (Life Technologies, Gaithersburg, MD, USA). RNA was quantified, and later, complementary DNA (cDNA) preparation was carried out. Approximately 1 µg of total RNA was reverse transcribed into cDNA using PrimeScript 1st strand cDNA Synthesis Kit (Takara Bio Inc., Shiga, Japan). Real-time quantitative polymerase chain reaction (PCR) was performed with Assays-on-demand (Applied Biosystems, USA) with primers Nrf2 forward primer 5′-TCTCCTCGCTGGAAAAAGAA-3′, reverse primer 5′-AATGTGCTGGCTGTGCTTTA-3′, GAPDH forward 5′-ACGGATTTGGTCGTATTGGGCG-3′, reverse primer 5′-CTCCTGGAAGATGGTGATGG-3.′ Each data point was repeated in triplicates. Quantification values were obtained using threshold PCR cycle number (Ct), where the increase in signal results in an increase in PCR product. The normalization of relative messenger RNA (mRNA) level in each sample was done with β-actin. The relative expression target gene levels equaled $\Delta Ct = Ct_{target\ gene} - Ct_{\beta-actin}$.

3-(4,5-Dimethylthiazol-2-yl)-2,5-diphenyltetrazolium bromide cell proliferation assay

Effect of different treatments of ganoderic acid A on the growth of lung cancer cells (H460) cells were assessed using the 3-(4,5-dimethylthiazol-2-yl)-2,5-diphenyltetrazolium bromide (MTT) assay in triplicates. Approximately, 10,000 cells were seeded in the 96-well plate in RPMI media containing 10% FBS and incubated 37°C overnight, followed by serum starvation for 24 h. Cells were treated with different concentrations of ganoderic acid A (5, 10, 20, 50, 80 µM/mL) in serum-free media which was incubated for 48 h. After, 48 h, the medium was replaced with 100 µL of MTT

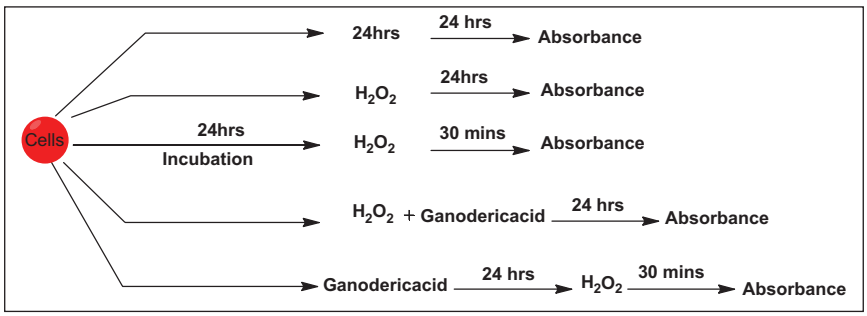

Figure 1. Schematic representation of strategies employed for the determination of ROS production by ganoderic acid.

(0.5 mg/mL in phosphate-buffered saline (PBS)) in 10% FBS containing media, and incubated at 37°C for 4 h in the dark. Then, the supernatant was removed and the reduced MTT, formazan complex, was solubilized in 200 µL/well DMSO. Absorbance was measured at 570 nm using microplate reader.

Evaluation of cytotoxic/apoptotic effect

The rate of cell death in response to ganoderic acid A with treatment was assessed for cytotoxic effect by trypan blue exclusion test. Around 2×10^5 H460 cells were seeded in six-well culture plates. The adhered cells were treated with ganoderic acid A (5, 10, 20, 50, 80 µM/mL) for 48 h. After treatment, both floating cells in the medium and adhered cells on the plate were collected and concentrated by centrifugation. The cell viability was estimated after staining with 0.4% trypan blue for 15 min. Both live (unstained) and dead (stained) cells were counted in three replicates using Automated Cell Counter (Invitrogen, India). Percent data of dead cells were calculated and used as an indicator of the degree of cell death.

Wound healing assay

H460 cells were seeded in a six-well plate and allowed to grow up to 75%–80% confluence level. The monolayer was scratched to form a wound, using a pipette tip, of 1.5 mm diameter. Subsequently, the cells were then washed twice with PBS to remove the detached cells. After that the cells were treated with different concentrations of the ganoderic acid A and incubated for 48 h. After this, the cells were monitored at different time intervals to observe their invasive behavior. Cell invasion into the wounded area was determined under Olympus inverted microscope (Olympus, Tokyo, Japan).

Nitro blue tetrazolium reduction assay

In this assay, superoxide ion production was measured by colorimetric nitro blue tetrazolium (NBT) assay which converts water-soluble NBT to water insoluble, NBT diformazan. Around 8×10^3 cells/well were seeded into the 96-well plates in RPMI media containing 10% FBS and 1% penicillin/streptomycin and then incubated at 37°C overnight followed by serum starvation for 24 h. After 24 h, the media was changed with fresh complete medium (200 µL) and exposed to different ganoderic acid concentrations (5, 10, 20, 40, and 80 µM). After 48 h, the medium was removed and incubated with 100 µL 0.1% NBT, incubated for 4 h. The reduced NBT was solubilized with 100 µL 2 M KOH and 100 µL DMSO for 30 min, and absorbance was taken at 570 nm.

Intracellular ROS assay

Around 10,000 cells were counted using trypan blue assay and seeded in 96 wells of the microtiter plate. Treatment strategies of ganoderic acid with hydrogen peroxide are represented in Figure 1. H460 cells were incubated for 24 h followed by treatment with compounds alone in different strategies. After the treatment, 10 mM of 2′,7′-dichlorodihydrofluorescein diacetate (H_2DCFDA) dye was used in the cultured cells and kept in the dark for 30 min, followed by absorbance at the emission wavelength of 530 nm.

Statistical analysis

The results were expressed as the mean ± standard deviation of experiments performed in triplicates. Data obtained were subjected to one-way analysis of variance (ANOVA), and significant differences of the mean were determined statistically using Tukey's test using SigmaPlot 11.

Results and discussion

Stress exacerbates cancer, cardiovascular disease, chronic inflammation, and neurodegenerative diseases.[29] To counteract the detrimental effects of stress, cells evolved the adaptive, dynamic, endogenous antioxidants by Nrf2 signaling mechanism. The activation of the cytoprotective enzyme by Nrf2 signaling provides the basis of chemopreventive and chemoprotective activities.[30] During stress conditions, phosphorylation of the cysteine residue in

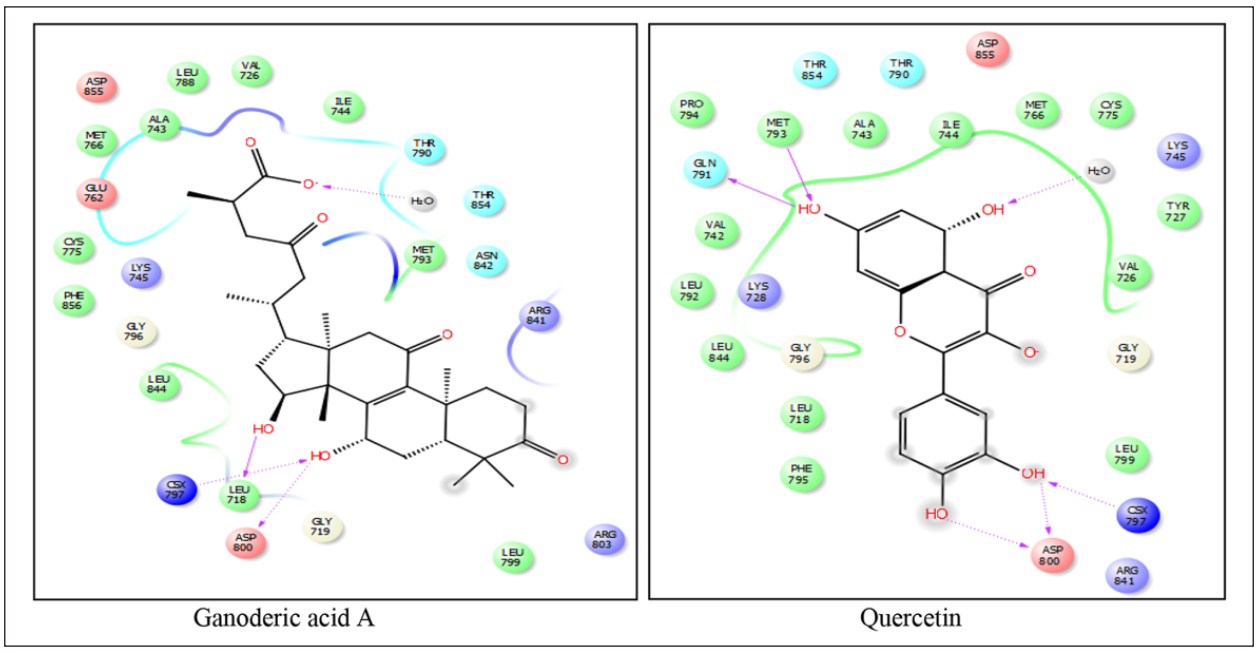

Figure 2. Interaction displayed in receptor-based molecular docking profile of Nrf2 (PDB: 4L7D) with ganoderic acid A and quercetin. Protein–ligand interactions involved in ganoderic acid A binding were Leu 718, Asp 800, and Cys 797, whereas Gln 791, Met 793, Asp 800, and Cys 797 were involved in quercetin.

Keap1 senses the cellular redox action. The oxidant modification in the cysteine residues results in transportation from cytoplasm to the nucleus. In addition to the decisive role of cysteine residues, serine or threonine is also considered important in the activation of Nrf2 signaling.[30] Among different protective agents targeting Nrf2, ganoderic acid along with its 50 isomers were docked using receptor-based molecular docking by Maestro 9.6 (Schrödinger Inc.). The molecular docking identifies the maximum energy, protein–ligand interactions, orientations, and conformations best suited for effective drug design.[31] Molecular docking predicts the best suitable fitted orientation to form a stable complex and finds the strength of association of binding affinity by different docking parameters.[17]

This study was carried out by ganoderic acid and its 50 isoforms which were docked with X-ray crystal structures of Nrf2 retrieved (PDB: 4L7D) from PDB. Triterpene of *G. lucidum*, ganoderic acid, has lanosterol scaffold, and variation in its isoforms varies in the functional group or in the side chain.[32] The binding interaction between receptors complexed with various isoforms of ganoderic acid highlighted the lipophilic, salt bridges, electrostatic, and hydrogen bonding interactions. In molecular docking of Nrf2, ganoderic acid A exhibits best docking parameters as GScore (−9.69), Lipophilic EvdW (−1.83), Glide emodel (73.369), and H Bond (−2.68), and hydrogen bonding forms basis of the stability of the complex. Different residues involved in hydrogen bonding were Leu 718, Asp 800, and Cys 797 with 2.45, 2.23, and 3.61 Å hydrogen bond length, respectively. Also, the stability of complex depends on activation of other covalent and non-covalent bindings, as shown in Figure 2. The binding affinity was calculated by MM-GBSA, which assesses the orientation of ligands to the receptors using scoring and thereby predicting binding interaction (Table 1).

The structure of ganoderic acid A has a tetracyclic ring with one double bond at a different position, and the branch ends with a carboxyl group while others with some modification. In molecular docking of ganoderic acid and its isoforms, –COOH group has a crucial role in different activities such as inhibitory effects, whereas –C=O or –OH group also has a role in signaling through different receptors. The lanosterol moieties in the ganoderic acid A have involvement of cysteine residue which leads to the activation and translocation of Nrf2 to the cytoplasm to the nucleus.

Among different natural activators, quercetin exhibits best-docked docking parameters with GScore (−7.8), Lipophilic EvdW (−4.69), Glide emodel (62.453), and Gln 791, Met 793, Asp 800, and Cys 797 residues participate in hydrogen bonding (Figure 1). The binding interaction of Nrf2 with quercetin exhibits participation of both phenyl and chromone moieties during docking process which makes it vital to design an effective drug. Different parameters of other isoforms and natural activators were presented in Table 1. The active participation of Cys and Ser residues during molecular docking assists in translocation and activation of different antioxidant genes in Nrf2 signaling pathway.

Table 1. Binding affinities, scores, and interaction of Nrf2 with different isoforms of ganoderic acid along with natural activators.

Ligand type	GScore (kcal/mol)	Lipophilic EvdW	H bond	Electro	Glide emodel	H-bond length (Å)	MM-GBSA (kcal/mol)	Protein–ligand interaction
Ganoderic acid A	−9.69	−1.83	−2.68	−1.1	−73.369	2.45, 2.23, 3.61	−75.541	Leu 718, Asp 800, Cys 797
Quercetin	−7.8	−4.69	−1.66	−0.22	−62.453	1.95, 2.48, 3.47	−76.782	Gln 791, Met 793, Asp 800, Cys 797
Ganoderic acid B methyl ester	−7.5	−3.23	−2.18	−0.66	−58.351	1.28, 3.17	−69.486	Asp 800, Met 793
Curcumin	−7.46	−2.53	−2.94	−1.08	−53.959	1.84, 1.87	−71.754	Glu 762, Met 793
Ganoderic acid alpha	−7.32	−3.22	−2.07	−0.64	−52.187	2.64, 2.44	−66.856	Asp 855, Met 793
Ganoderic acid B	−6.63	−2.7	−2.26	−1.25	−55.929	2.86, 3.74	−63.111	Asp 800, Met 793
Ganoderic acid R	−6.15	−3.28	−1.02	−0.44	−52.760	3.53, 1.92	−55.986	Met 793, Cys 797
Ganodermic acid S	−6.15	−3.28	−1.02	−0.44	−52.760	3.73, 2.66	−61.321	Met 793, Cys 797
Methyl ganoderate D	−6.06	−2.45	−1.53	−0.85	−58.391	3.37, 2.55	−54.335	Asp 800, Met 793
Ganoderic acid Mk	−5.97	−2.79	−1.88	−1.27	−53.144	1.83, 1.48	−60.482	Ser 720, Asp 855
Withaferin A	−5.97	−2.62	−1.84	−0.68	−36.771	2.36	−67.132	Met 793
Ganoderic acid G	−5.95	−2.34	−2.36	−1.01	−54.905	2.58, 3.48	−57.545	Asp 800, Met 793
Ganoderiol B	−5.67	−3.17	−2.32	−0.6	−48.173	1.03, 3.43, 2.67	−47.892	Gln 791, Asp 855, Cys 797
Ganoderic acid D	−5.54	−2.62	−1.58	−1.04	−55.934	3.01, 1.45	−51.333	Met 793, Ser 720
Ganoderic acid F	−5.53	−3.31	−1.37	−0.62	−59.390	3.54, 2.47	−45.574	Met 793, Lys 745
Ganoderiol A	−5.48	−3.18	−2.26	−0.36	−41.420	2.38	−42.662	Met 793
Ganoderic acid DF	−5.38	−2.53	−1.65	−1.08	−57.976	3.63, 1.82, 3.68	−48.578	Met 793, Ser 720, Asp 800
Ganoderic acid K	−5.32	−2.32	−1.45	−1.19	−55.370	2.33, 2.62	−40.161	Asp 800, Met 793
Lucidenic acid P	−5.31	−2.5	−2.07	−0.79	−51.985	2.59, 3.82, 3.21	−47.651	Asp 800, Met 793, Cys 797
Ganoderic acid C2	−5.24	−1.76	−2.78	−1.1	−49.137	1.93, 2.88, 1.62	−44.568	Asp 855, Lys 875, Gly 724
Ganoderic acid G	−5.24	−2.07	−2.38	−1.13	−45.663	1.99, 2.39, 2.83	−44.143	Asp 855, Gly 724, Ser 720
Ganoderic acid C1	−5.19	−2.49	−1.53	−0.87	−47.842	3.75	−43.887	Met 793
Ganoderic acid D	−5.15	−2.25	−1.67	−0.81	−49.868	3.77, 3.62	−42.798	Asp 800, Met 793
Ganoderic acid Lm2	−5.15	−3.43	−1.32	−0.4	−41.520	2.58, 2.49	−42.452	Asp 800, Lys 745
Ganoderic acid J	−4.83	−2.29	−1.61	−0.79	−50.766	3.42, 2.79, 2.38	−39.756	Met 793, Gly 724, Asn 842
Ganodermanontriol	−4.81	−2.13	−3.22	−1.1	−45.019	2.69	−38.955	Asp 800
Ganolucidic acid A	−4.8	−2.92	−0.97	−0.7	−52.208	2.75, 2.56	−38.342	Met 793, Asp 855
Ganoderic acid Me	−4.76	−2.13	−1.62	−0.82	−49.494	3.82, 3.35	−37.456	Met 793, Ser 720
Ganoderic acid theta	−4.72	−3.16	−1.78	−0.84	−45.795	3.46, 2.51, 4.21	−36.445	Met 793, Gly 724, Lys 745
Lucialdehyde B	−4.66	−2.94	−0.7	−0.14	−42.771	2.34, 2.29	−34.879	Met 793, Cys 797
Ganosporeric acid A	−4.64	−2.4	−1.39	−0.67	−47.523	3.07	−34.751	Met 793
Lucidenic acid A	−4.63	−2.33	−1.73	−0.63	−41.558	3.94	−33.555	Met 793
Ganodermanontriol	−4.61	−2.32	−2.09	−0.66	−42.917	2.46, 3.62, 2.44	−32.289	Asn 842, Asp 855, Cys 797
Ganoderic acid X	−4.54	−3.42	−0.67	−0.6	−57.373	2.48, 3.88	−31.567	Met 793, Gly 724
Ganolucidic acid E	−4.52	−2.77	−1.04	−0.84	−44.244	1.66, 2.68	−31.198	Asp 855, Met 793
Ganoderol B	−4.51	−3.21	−1.28	−0.4	−37.225	2.46	−31.198	Gly 724
Ganoderic acid E	−4.5	−2.96	−0.97	−0.34	−44.178	2.61	−31.188	Lys 745
Ganoderic acid C6	−4.52	−2.21	−1.82	−1.02	−48.100	3.87, 1.83, 1.47	−31.077	Lys 745, Ser 720, Gly 724
Ganoderic acid Am1	−4.43	−2.59	−1.1	−0.58	−48.992	2.91	−30.452	Met 793
Lucidenic acid C	−4.4	−1.7	−2.02	−0.95	−40.849	2.58	−29.468	Asp 855
Ganoderic acid S	−4.39	−3.57	−0.56	−0.46	−35.879	2.97	−36.148	Met 793
Lucialdehyde C	−4.28	−3.33	−0.77	−0.28	−43.463	3.39, 2.59	−35.689	Met 793, Lys 745
Ganodermatriol	−4.28	−2.33	−2.55	−0.86	−45.933	1.83, 1.62	−28.781	Pro 794, Cys 797

Table 1. (Continued)

Ligand type	GScore (kcal/mol)	Lipophilic EvdW	H bond	Electro	Glide emodel	H-bond length (Å)	MM-GBSA (kcal/mol)	Protein–ligand interaction
Ganoderiol F	−4.24	−3.37	−1.12	−0.23	−31.968	2.34	−28.286	Met 793
Tirucallol	−3.84	−3.31	−0.7	−0.2	−30.260	2.55, 1.92	−33.587	Ser 720, Met 793
Ganoderic acid TR	−3.83	−3.01	−0.33	−0.44	−37.438	3.22, 3.88	−27.678	Met 793, Cys 797
Ganolucidic acid B	−3.81	−2.45	−0.7	−0.31	−45.007	2.44	−25.558	Gly 724
Ursolic acid	−3.8	−2.84	−0.67	−0.35	−46.594	3.17	−32.717	Met 793
Ganoderic acid Sz	−3.71	−2.59	−0.7	−0.53	−39.549	3.57	−31.469	Met 793
Ganoderic acid T-Q	−3.67	−2.83	−0.35	−0.28	−47.952	3.29	−26.764	Met 793
Ganoderic acid TR1	−3.67	−2.7	−1.24	−0.79	−40.217	2.66, 3.44	−22.875	Asp 800, Met 793
Ganoderic acid H	−3.67	−2.8	−1.36	−0.64	−48.762	2.05, 2.46	−22.783	Met 793, Cys 797
Betulinic acid	−3.61	−2.83	−0.51	−0.27	−39.585	1.98	−22.736	Asp 855
Ganoderic acid Y	−3.37	−3.26	0	−0.11	−37.480	3.58, 2.63	−21.888	Lys 745, Asn 842
Ganoderic acid beta	−3.26	−2.26	−0.35	−0.42	−39.019	1.88	−21.652	Asn 842
Ganoderic acid DM	−3.25	−2.55	−0.3	−0.29	−39.400	3.25	−21.045	Met 793
Pristimerin	−2.82	−2.38	−0.48	0.06	−44.423	3.66	−29.826	Met 793
Celastrol	−2.75	−2.17	−0.48	0	−31.543	3.27	−26.444	Met 793
Ganoderic acid T	−2.44	−3.36	−1.34	−0.32	−61.022	3.19	−19.118	Lys 745

ADME properties

Binding affinity prediction is useful for analyzing the pharmacokinetic and pharmacodynamic properties. ADME-T predicts physicochemical, effective permeability in jejunum, blood–brain barrier permeation, pKa (ionization constants a multi-protic model), intrinsic clearance solubility, toxicity risks, optimal dose in human, fraction absorbed in human, likely sites of metabolic attack, logD, logP, and MDCK apparent permeability. QikProp is an important tool that calculates properties of the valid descriptors and pharmaceutically relevant molecules by comparing their values with those of 95% of already known pharmaceutical drugs. Ganoderic acid and its 50 isoforms were checked for ADME-T properties. Most interesting aspects of these compounds are their admirable QPlogPo/w, QPlogHERG K+ channels, QPlogBB, QPlogKP, and QPlogKhsa values that satisfy Lipinski's rule of five (Table 2). Some of the isomers in different receptors did not satisfy all aspects and needed some modifications in the basic lanosterol structure (Table 2). Predicted IC50 value for blockage of HERG K+ channels (acceptable range: above −5.0); QPP Caco—predicted apparent Caco-2 cell permeability in nm/s. Caco-2 cell is a model for the gut–blood barrier (nm/s) (<25: poor, >500: great); QPlogBB—predicted brain/blood partition coefficient; QPP MDCK—predicted apparent MDCK cell permeability in nm/s. MDCK cells are considered to be a good mimic for the blood–brain barrier (nm/s) (<25: poor, >500: great); QPlogKP—predicted skin permeability; percentage of human oral absorption (<25% is poor and >80% is high).

Effects of ganoderic acid A on cancer cells

The cytotoxicity of ganoderic acid A in cancer cells was performed by MTT assay. Lung cancer cells H460 were treated with different concentrations (5, 10, 20, 50, 80 μM) of ganoderic acid A at different time intervals (24, 48, and 72 h). Ganoderic acid A marked 50% of inhibition at 50 μM and higher concentration and best marked in 48 h. Ganoderic acid A exhibited a remarkable reduction in cell proliferation in cancer cells in a concentration-dependent manner (Figure 3(a)).

Cell viability was checked by trypan blue exclusion test to determine the number of the treatments of ganoderic acid A. Treatment of ganoderic acid A in H460 cells with different concentrations (5, 10, 20, 50, 80 μM) for the duration of 48 h displayed a reduction in cell viability to exactly 32%, 36%, 44%, 51%, and 55%, respectively (Figure 3(b)). Thus, it can be concluded that ganoderic acid reduced cell viability in a concentration-dependent manner. Furthermore, NBT assay (colorimetric method) was used to analyze the antioxidant potential of ganoderic acid A, which converts tetrazolium chloride to diformazan by superoxide production. Ganoderic acid A causes a reduction in ROS to 50% in 50 μM and higher concentration in NBT reduction assay (Figure 3(c)). Furthermore, treatment of ganoderic acid inhibits the migration of H460 cells in a dose-dependent manner after 48 h. Photomicrographs of H460 cells are represented in Figure 4(a), in which cell migration was analyzed after 48 h as compared to control. Treatment with ganoderic acid (10, 20, and 50 μM) reduced the migration and increased the wound in dose-dependent manner (Figure 4). Thus, this study concludes that ganoderic acid A has potential to inhibit proliferation, viability, and ROS in the H460 cells.

Antioxidant potential of ganoderic acid

The ROS production potential of ganoderic acid A was evaluated by DCFDA strategies represented in Figure 1.

Table 2. Evaluation of drug-like properties of the different isoforms of ganoderic acid and another natural activator of Nrf2 by QikProp.

Molecule	Molecular weight	Dipole	QPlogPo/w (−2.0 to 6.5)	QPlogHERG K+ (acceptable range: above −5.0)	QPP Caco (nm/s) (<25: poor; >500: great)	QPlogBB (−3 to 1.2)	QPP MDCK (nm/s)	QPlogKP (−8.0 to −0.1)
Ganoderic acid A	516.673	5.026	2.857	−2.383	121.188	−2.006	9.761	−4.781
Quercetin	304.256	5.749	0.155	−4.691	25.299	−2.179	9.296	−5.369
Ganoderic acid B methyl ester	528.684	3.711	2.883	−4.2	140.607	−1.77	59.353	−4.312
Curcumin	368.385	6.085	2.74	−6.157	150.697	−2.218	63.97	−3.019
Ganoderic acid alpha	574.71	6.656	2.412	−1.805	13.488	−2.08	5.991	−5.066
Ganoderic acid B	516.673	6.114	2.64	−2.13	12.076	−2.167	5.316	−5.256
Ganoderic acid R	554.765	6.343	6.876	−3.063	48.152	−1.743	23.705	−4.105
Ganodermic acid S	554.765	6.343	6.876	−3.063	48.152	−1.743	23.705	−4.105
Methyl ganoderate D	528.684	5.61	2.761	−3.953	142.155	−1.65	60.06	−4.43
Ganoderic acid Mk	556.738	11.276	5.677	−2.377	73.067	−1.429	37.205	−3.624
Withaferin A	470.605	9.527	2.998	−4.524	215.095	−1.401	93.973	−3.993
Ganoderic acid G	532.673	7.787	1.941	−2.312	9.872	−2.375	4.276	−5.329
Ganoderiol B	470.691	3.719	4.446	−4.19	449.777	−1.297	208.584	−3.138
Ganoderic acid D	514.658	5.132	2.698	−2.298	14.136	−2.094	6.302	−5.219
Ganoderic acid F	570.678	6.81	2.426	−2.457	12.918	−2.187	5.718	−5.294
Ganoderiol A	474.723	2.284	4.601	−4.296	510.016	−1.328	238.937	−2.952
Ganoderic acid DF	516.673	3.919	2.624	−1.935	16.481	−1.977	7.44	−4.993
Ganoderic acid K	574.71	7.143	2.537	−2.383	8.517	−2.465	3.645	−5.454
Lucidenic acid P	518.646	3.263	2.612	−2.4	13.702	−2.142	6.094	−5.245
Ganoderic acid C2	518.689	9.69	2.729	−2.471	9.22	−2.462	3.971	−5.387
Ganoderic acid G	532.673	6.978	1.814	−1.993	14.126	−2.118	6.298	−5.027
Ganoderic acid C1	514.658	6.53	2.791	−1.914	19.115	−1.85	8.733	−4.964
Ganoderic acid D	514.658	7.941	2.968	−2.262	18.895	−1.958	8.624	−4.974
Ganoderic acid Lm2	514.658	6.148	2.671	−2.57	9.392	−2.358	4.051	−5.54
Ganoderic acid J	514.658	5.909	2.67	−2.395	11.454	−2.219	5.021	−5.396
Ganodermanontriol	472.707	6.122	5.253	−4.558	973.346	−1.03	480.472	−2.518
Ganolucidic acid A	500.674	7.426	3.549	−2.191	18.221	−1.952	8.292	−5.004
Ganoderic acid Me	554.765	7.461	6.869	−3.11	39.632	−1.844	19.206	−4.253
Ganoderic acid theta	530.657	4.432	1.902	−2.367	6.723	−2.487	2.823	−5.722
Lucialdehyde B	452.676	6.543	5.21	−4.305	483.04	−1.071	225.306	−3.55
Ganosporeric acid A	526.625	6.827	1.679	−2.8	5.508	−2.647	2.276	−6.11
Lucidenic acid A	458.594	5.109	2.637	−2.067	16.669	−1.831	7.532	−5.272
Ganodermanontriol	472.707	4.935	4.735	−4.258	328.383	−1.453	148.462	−3.428
Ganoderic acid X	512.728	3.461	6.364	−2.619	124.806	−1.192	66.363	−3.286
Ganolucidic acid E	484.675	7.702	4.531	−2.271	34.347	−1.631	16.454	−4.532
Ganoderol B	440.708	3.847	5.872	−4.403	1542.05	−0.672	790.064	−2.266
Ganoderic acid E	512.642	3.654	2.57	−2.539	14.653	−2.099	6.552	−5.284
Ganoderic acid C6	530.657	6.914	2.016	−2.411	13.094	−2.226	5.802	−5.187
Ganoderic acid Am1	514.658	3.074	2.829	−2.291	17.218	−2.007	7.8	−5.052
Lucidenic acid C	476.609	5.151	2.022	−1.845	19.388	−1.825	8.868	−4.952
Ganoderic acid S	452.676	2.325	6.358	−2.347	159.321	−0.906	86.405	−3.234
Lucialdehyde C	468.718	4.931	5.342	−3.843	586.581	−1.017	277.933	−3.164
Ganodermatriol	456.707	3.651	5.403	−4.383	690.294	−1.144	331.409	−2.765
Ganoderiol F	454.692	2.676	5.395	−4.521	712.293	−1.096	342.84	−2.841
Tirucallol	426.724	1.507	7.501	−4.17	4414.254	−0.086	2462.433	−1.662
Ganoderic acid TR	468.675	2.997	5.595	−2.698	98.398	−1.239	51.325	−3.532
Ganolucidic acid B	502.69	4.369	3.637	−2.456	15.127	−2.177	6.781	−5.065
Ursolic acid	456.707	1.629	5.774	−1.599	308.445	−0.367	176.461	−3.037
Ganoderic acid Sz	452.676	5.688	6.344	−2.549	120.848	−1.054	64.091	−3.441
Ganoderic acid T-Q	510.712	10.499	6.316	−2.544	121.725	−1.121	64.594	−3.379
Ganoderic acid TR1	468.675	7.763	5.235	−2.42	61.528	−1.387	30.897	−3.945
Ganoderic acid H	572.694	5.667	2.684	−2.802	11.15	−2.44	4.877	−5.323
Betulinic acid	456.707	2.628	6.135	−2.287	327.218	−0.484	188.098	−2.886

Table 2. (Continued)

Molecule	Molecular weight	Dipole	QPlogPo/w (−2.0 to 6.5)	QPlogHERG K+ (acceptable range: above −5.0)	QPP Caco (nm/s) (<25: poor; >500: great)	QPlogBB (−3 to 1.2)	QPP MDCK (nm/s)	QPlogKP (−8.0 to −0.1)
Ganoderic acid Y	454.692	2.598	6.442	−2.805	115.839	−1.187	61.225	−3.39
Ganoderic acid beta	484.675	4.92	4.58	−2.386	56.411	−1.451	28.129	−4.124
Ganoderic acid DM	468.675	7.039	5.62	−2.36	117.483	−1.063	62.164	−3.589
Pristimerin	464.644	7.559	5.373	−4.289	608.198	−0.737	289.02	−3.444
Celastrol	450.617	7.561	4.925	−1.955	77.702	−0.934	39.763	−4.073
Ganoderic acid T	612.802	6.505	6.104	−3.139	12.885	−2.452	5.702	−5.105

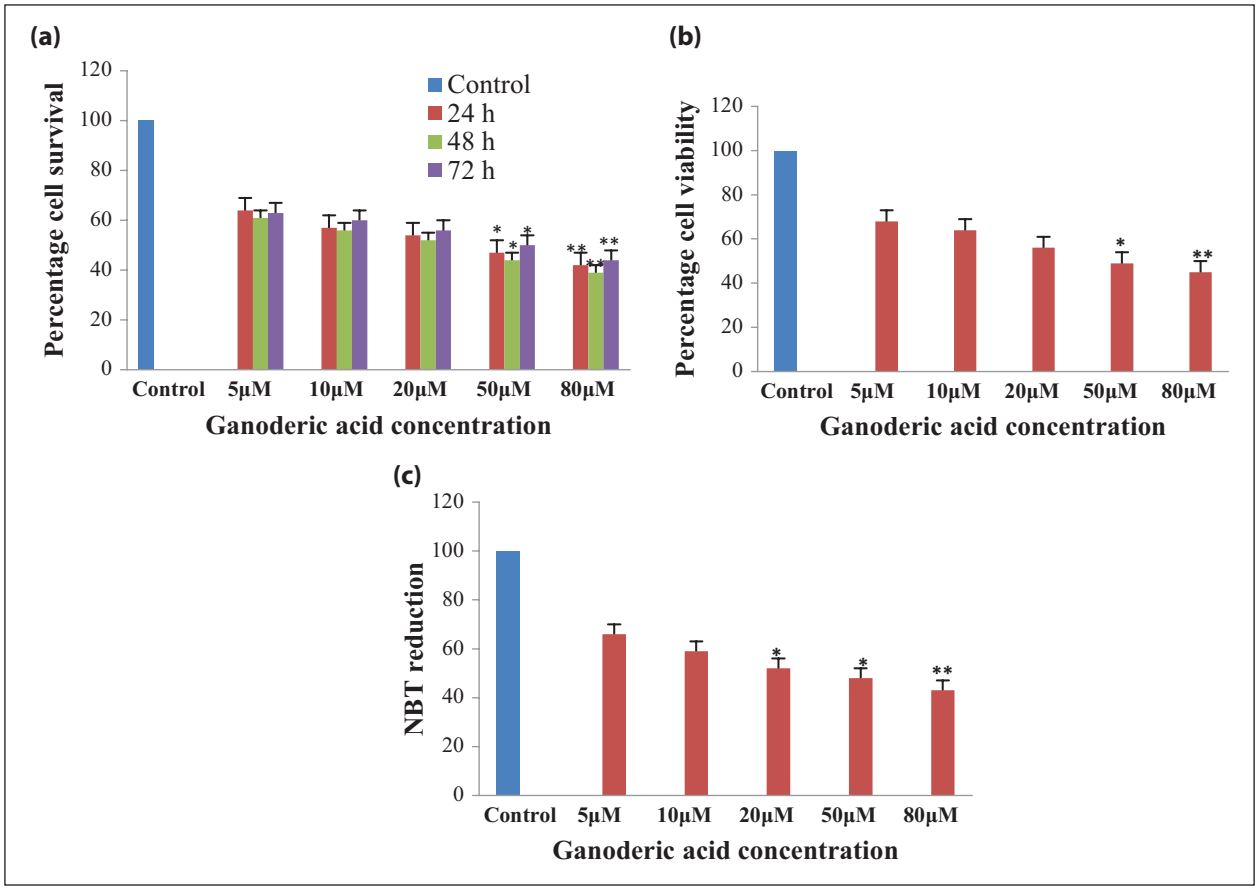

Figure 3. Effect of ganoderic acid A on H460 cells. (a) Ganoderic acid A reduces the cell growth in a dose-dependent manner determined by the MTT assay, (b) reduces the cell number of H460 cells in a dose-dependent manner determined by the trypan blue exclusion test of the cell, (c) significantly reduces the cell number of H460 cells in a dose-dependent manner determined by the NBT reduction assay.
*$p < 0.05$ and **$p < 0.01$ versus control.

Different treatments in H460 cells with different concentrations of ganoderic acid A make them to behave differently. Cell treatment with H_2O_2 increases free radicals, whereas ganoderic acid scavenges free radicals and enhances antioxidant potential in dose-dependent manner (20, 50, and 80 μM). Potential of ganoderic acid enhances more efficiently when H_2O_2 treatment was given for 24 h as compared to treatment of H_2O_2 given for 30 min after 24 h of cells treatment. Thus, it was inferred that ganoderic acid shows antioxidant potential when H_2O_2 was given in time-dependent manner (Figure 5).

Effect of ganoderic acid A on Nrf2 mRNA expression in H460 cells

The effect of ganoderic acid A on Nrf2 mRNA expression was determined using quantitative polymerase chain reaction (qPCR). The results show that ganoderic acid A has

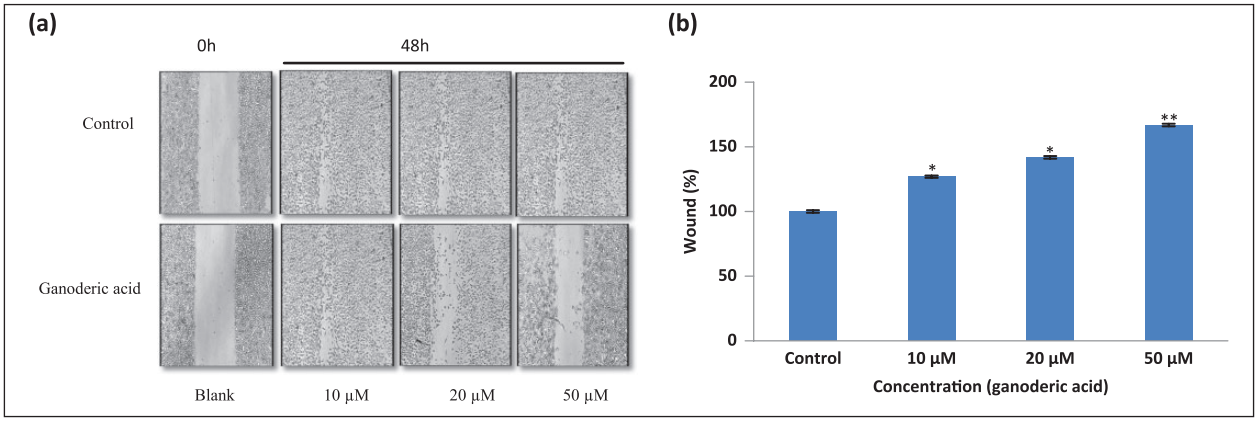

Figure 4. Ganoderic acid A reduces the cell migration in H460 cells determined by wound healing assay. (a) H460 cells treated with different concentrations (10, 20, and 50 µM) of ganoderic acid A are presented with photomicrographs. Cells were seeded in six-well plate and grown overnight, and next day, scratch was made in confluent monolayer, followed by treatment with ganoderic acid for 48 h. (b) The rate of wound closure was analyzed using ImageJ and exhibiting the increase in width of wound after ganoderic acid treatment.
*$p < 0.05$; **$p < 0.01$; and ***$p < 0.001$ versus control.

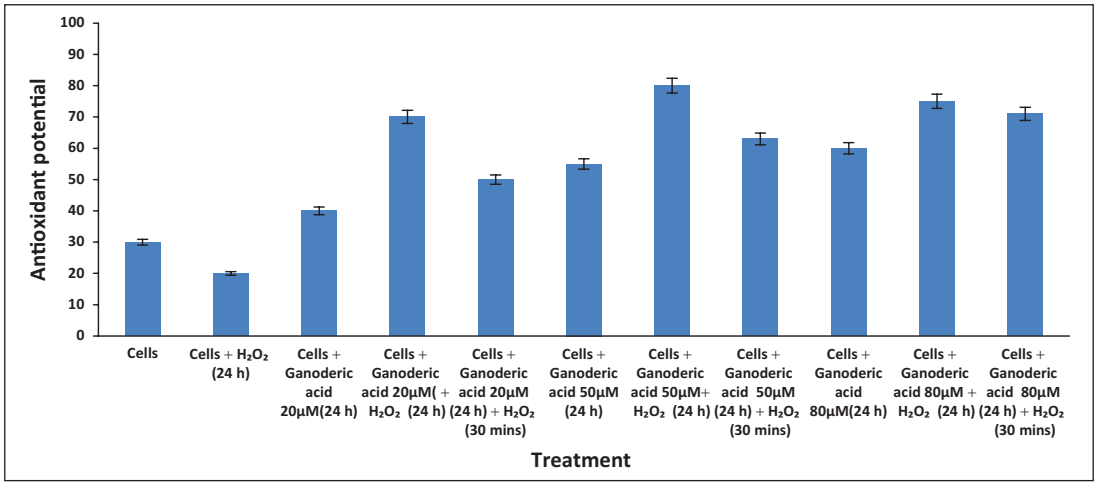

Figure 5. Graphical representation of antioxidant potential of ganoderic acid in different strategies with hydrogen peroxide (H_2O_2) in the dose- and time-dependent manner.

the potential to reduce the Nrf2 rnRNA expression in H460 cells. The natural inhibitor, quercetin, treatment decreases the Nrf2 mRNA expression by 29%, whereas ganoderic acid A decreases by 22.5% at 80 µM concentration in H460 cells (Figure 6).

Conclusion

Nature fulfilled the need of humanity by rich flora and fauna with an inexhaustible reservoir of the natural products. *Ganoderma lucidum* and its bioconstituents effectively target the expression of numerous signaling proteins in cancer. Various isoforms of ganoderic acid comprise of lanosterol moieties, and variation in its isoforms varies in the side chains or the functional groups. Nrf2 signaling protects from free radicals by activating various antioxidants genes and unbalances in free radicals scavenging forms the cause of the various diseases. This study shows receptor-based molecular docking of Keap1-Nrf2 endowed with an in-depth understanding of docking interaction which assists in designing effective drugs. The active participation of cysteine and serine residues in activation and translocation of the Keap1-Nrf2 pathway in docking with ganoderic acid A highlighted its effectiveness during the process. Ganoderic acid A effectively inhibits cell proliferation, viability, ROS, and mRNA expression of Nrf2 expression in H460 cells and thus provides the platforms to target Nrf2 signaling, but more exploration is still needed in this field. Our present group is engaged in determining the anticancer property of *G. lucidum* and its bioconstituents.

Acknowledgements

The authors thank Central University of Punjab, Bathinda, for providing the necessary facilities to carry out this work.

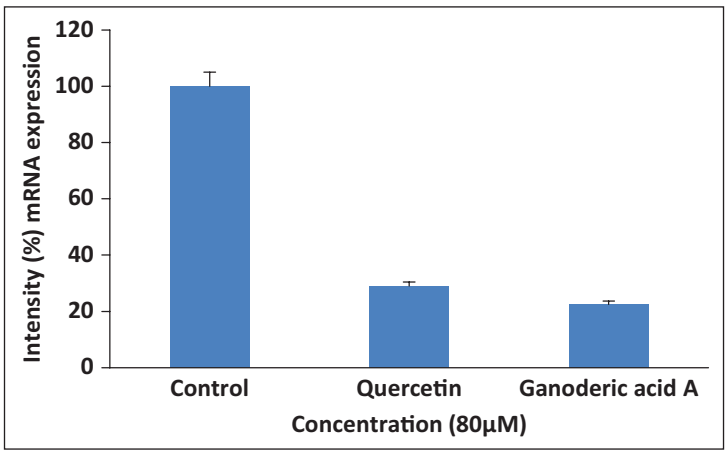

Figure 6. Expression analysis of ganoderic acid A and quercetin in qPCR at 80 μM. Natural inhibitor of Nrf2, quercetin, inhibits the mRNA expression (29%), whereas ganoderic acid A inhibits expression (22%) at 80 μM in H460 cells as compared to control.

Declaration of conflicting interests

The author(s) declared no potential conflicts of interest with respect to the research, authorship, and/or publication of this article.

Funding

The author(s) received no financial support for the research, authorship, and/or publication of this article.

References

1. Schieber M and Chandel NS. ROS function in redox signaling and oxidative stress. *Curr Biol* 2014; 24(10): R453–R462.
2. Itoh K, Wakabayashi N, Katoh Y, et al. Keap1 represses nuclear activation of antioxidant responsive elements by Nrf2 through binding to the amino-terminal Neh2 domain. *Genes Dev* 1999; 13(1): 76–86.
3. Kansanen E, Kuosmanen SM, Leinonen H, et al. The Keap1-Nrf2 pathway: mechanisms of activation and dysregulation in cancer. *Redox Biol* 2013; 1(1): 45–49.
4. Itoh K, Chiba T, Takahashi S, et al. An Nrf2/small Maf heterodimer mediates the induction of phase II detoxifying enzyme genes through antioxidant response elements. *Biochem Biophys Res Commun* 1997; 236(2): 313–322.
5. Shibutani S, Takeshita M and Grollman AP. Insertion of specific bases during DNA synthesis past the oxidation-damaged base 8-oxodG. *Nature* 1991; 349(6308): 431–434.
6. Jaramillo MC and Zhang DD. The emerging role of the Nrf2–Keap1 signaling pathway in cancer. *Genes Dev* 2013; 27(20): 2179–2191.
7. Yao P, Nussler A, Liu L, et al. Quercetin protects human hepatocytes from ethanol-derived oxidative stress by inducing heme oxygenase-1 via the MAPK/Nrf2 pathways. *J Hepatol* 2007; 47(2): 253–261.
8. Farombi EO, Shrotriya S, Na H-K, et al. Curcumin attenuates dimethylnitrosamine-induced liver injury in rats through Nrf2-mediated induction of heme oxygenase-1. *Food Chem Toxicol* 2008; 46(4): 1279–1287.
9. Li L, Zhang X, Cui L, et al. Ursolic acid promotes the neuroprotection by activating Nrf2 pathway after cerebral ischemia in mice. *Brain Res* 2013; 1497: 32–39.
10. Seo WY, Goh AR, Ju SM, et al. Celastrol induces expression of heme oxygenase-1 through ROS/Nrf2/ARE signaling in the HaCaT cells. *Biochem Biophys Res Commun* 2011; 407(3): 535–540.
11. Gill BS and Kumar S. Triterpenes in cancer: significance and their influence. *Mol Biol Rep* 2016; 43(9): 881–896.
12. Gill BS, Sharma P and Kumar S. Chemical composition and antiproliferative, antioxidant, and proapoptotic effects of fruiting body extracts of the Lingzhi or Reishi medicinal mushroom, *Ganoderma lucidum* (Agaricomycetes), from India. *Int J Med Mushrooms* 2016; 18(7): 599–507.
13. Gill B, Sharma P, Kumar R, et al. Misconstrued versatility of *Ganoderma lucidum*: a key player in multi-targeted cellular signaling. *Tumor Biol* 2016; 37(3): 2789–2804.
14. Gill BS and Kumar S. Evaluating anti-oxidant potential of ganoderic acid A in STAT 3 pathway in prostate cancer. *Mol Biol Rep* 2016; 43(12): 1411–1422.
15. Gill BS and Kumar S. Ganoderic acid targeting multiple receptors in cancer: in silico and in vitro study. *Tumor Biol* 2016; 37(10): 14271–14290.
16. Gill BS and Kumar S. Ganoderic acid A targeting β-catenin in Wnt signaling pathway: in silico and in vitro study. *Interdiscipl Sci*. Epub ahead of print 22 August 2016. DOI: 10.1007/s12539-016-0182-7.
17. Anand SS and Gill BS. Breakthroughs in epigenetics. *PharmaTutor* 2015; 3(7): 16–24.
18. Jnoff E, Albrecht C, Barker JJ, et al. Binding mode and structure-activity relationships around direct inhibitors of the Nrf2-Keap1 complex. *ChemMedChem* 2014; 9(4): 699–705.
19. Jorgensen WL, Maxwell DS and Tirado-Rives J. Development and testing of the OPLS all-atom force field on conformational energetics and properties of organic liquids. *J Am Chem Soc* 1996; 118(45): 11225–11236.
20. Jorgensen WL and Tirado-Rives J. The OPLS [optimized potentials for liquid simulations] potential functions for proteins, energy minimizations for crystals of cyclic peptides and crambin. *J Am Chem Soc* 1988; 110(6): 1657–1666.
21. Shivakumar D, Williams J, Wu Y, et al. Prediction of absolute solvation free energies using molecular dynamics free energy perturbation and the OPLS force field. *J Chem Theory Comput* 2010; 6(5): 1509–1519.

22. Singh P and Bast F. Screening and biological evaluation of myricetin as a multiple target inhibitor insulin, epidermal growth factor, and androgen receptor; in silico and in vitro. *Invest New Drugs* 2015; 33(3): 575–593.
23. Repasky MP, Shelley M and Friesner RA. Flexible ligand docking with Glide. *Curr Protoc Bioinformatics* 2007; 18: 8.12. DOI: 10.1002/0471250953.bi0812s18.
24. Friesner RA, Banks JL, Murphy RB, et al. Glide: a new approach for rapid, accurate docking and scoring. 1. Method and assessment of docking accuracy. *J Med Chem* 2004; 47(7): 1739–1749.
25. Friesner RA, Murphy RB, Repasky MP, et al. Extra precision glide: docking and scoring incorporating a model of hydrophobic enclosure for protein-ligand complexes. *J Med Chem* 2006; 49(21): 6177–6196.
26. Sitkoff D, Sharp KA and Honig B. Accurate calculation of hydration free energies using macroscopic solvent models. *J Phys Chem* 1994; 98(7): 1978–1988.
27. Lyne PD, Lamb ML and Saeh JC. Accurate prediction of the relative potencies of members of a series of kinase inhibitors using molecular docking and MM-GBSA scoring. *J Med Chem* 2006; 49(16): 4805–4808.
28. Jorgensen WL and Duffy EM. Prediction of drug solubility from structure. *Adv Drug Deliv Rev* 2002; 54(3): 355–366.
29. Gill B, Alex J and Kumar S. Missing link between microRNA and prostate cancer. *Tumour Biol* 2016; 37(5): 5683–5704.
30. Surh YJ, Kundu JK and Na H-K. Nrf2 as a master redox switch in turning on the cellular signaling involved in the induction of cytoprotective genes by some chemopreventive phytochemicals. *Planta Med* 2008; 74(13): 1526–1539.
31. Negi A and Gill BS. Success stories of enolate form of drugs. *PharmaTutor* 2013; 1(2): 45–53.
32. Gill BS and Kumar S. Differential algorithms-assisted molecular modeling-based identification of mechanistic binding of ganoderic acids. *Med Chem Res* 2015; 24(9): 3483–3493.